



Contents lists available at ScienceDirect

Saudi Pharmaceutical Journal

journal homepage: www.sciencedirect.com



Original article

Evaluation of burn wound healing activity of novel fusidic acid loaded microemulsion based gel in male Wistar albino rats

Mehmet Evren Okur^a, Şule Ayla^b, Vildan Yozgatlı^c, Neşe Buket Aksu^d, Ayşegül Yoltaş^e, Duygu Orak^{f,g}, Hande Sipahi^f, Neslihan Üstündağ Okur^{h,*}^aUniversity of Health Sciences, Faculty of Pharmacy, Department of Pharmacology, İstanbul, Turkey^bIstanbul Medipol University, School of Medicine, Department of Histology and Embryology, Beykoz, 34810 İstanbul, Turkey^cEge University, Faculty of Pharmacy, Department of Pharmaceutical Technology, Bornova, 35100 İzmir, Turkey^dAltınbaş University, School of Pharmacy, Department of Pharmaceutical Technology, 34217 İstanbul, Turkey^eEge University, Faculty of Science, Department of Biology, Fundamental and Industrial Microbiology Division, Bornova, İzmir, Turkey^fYeditepe University, Faculty of Pharmacy, Department of Toxicology, İstanbul, Turkey^gYeditepe University, Faculty of Engineering, Genetics and Bioengineering Department, İstanbul, Turkey^hUniversity of Health Sciences, Faculty of Pharmacy, Department of Pharmaceutical Technology, İstanbul, Turkey

ARTICLE INFO

Article history:

Received 7 April 2019

Accepted 29 January 2020

Available online 3 February 2020

Keywords:

Fusidic acid

In vivo burn treatment

Microemulsion based gel

Cell culture

Rat

Anti-inflammatory activity

ABSTRACT

The objective of the present research was to examine the possible usage of microemulsion based gel for fusidic acid (FA) dermal application as burn wound treatment. During the preparation of microemulsion, ethyl oleate as oil phase, tween 80 as a surfactant, ethanol as co-surfactant, water as aqueous phase were used. The prepared microemulsions were evaluated for clarity, pH, viscosity and FA content. Moreover, stability, sterility, antibacterial activity, *in vitro* release of the formulations were also evaluated. The results showed that the FA loaded microemulsion and microemulsion based gel formation and characteristics were related to many parameters of the components. The performed optimized microemulsion-based gel showed good stability over a period of 3 months. The antibacterial activity of microemulsion-based gel was found to be comparable with marketed cream. RAW 264.7 macrophages were used to determine cell viability (MTT assay) and nitric oxide production. MBG and FA-MBG significantly inhibit the production of the inflammatory mediator NO in LPS-stimulated RAW 264.7 cells in a concentration-dependent manner. The wound healing property was evaluated by histopathological examination and by measuring the wound contraction. The % of wound area in rats treated with FA (2%) loaded microemulsion based gel ranged from 69.30% to 41.39% in the period from 3 to 10 days. In conclusion, FA loaded microemulsion based gel could be offered as encouraging strategy as dermal systems for the burn wound treatment.

© 2020 The Authors. Published by Elsevier B.V. on behalf of King Saud University. This is an open access article under the CC BY-NC-ND license (<http://creativecommons.org/licenses/by-nc-nd/4.0/>).

1. Introduction

A burn is defined as damage to the skin caused by excessive heat or caustic chemicals. The most common burn injuries result from exposure to heat and chemicals (Trabelsi et al., 2017). Burns

is a prevalent and burdensome critical care problem (Rowan et al., 2015). The depth of a burn wound and/or its healing potential are the most important factors of the therapeutic management and the residual morbidity or scarring (Monstrey et al., 2008). Wound healing is an active and dynamic process that begins from the moment of injury. Any delay in the initiation of the response to injury can prolong the healing process (Gurel et al., 2015).

Microorganisms that cause burn wound infections have changed over years related to changes made in the treatment of burn patients. Infection is a major complication of burn injury and is responsible for 50–75% of hospital deaths (Dua et al., 2013). Many of the antimicrobial agents are designed to be used prophylactically to prevent infection developing, while others are designed to kill the microbial cells that are proliferating within the burn

* Corresponding author at: University of Health Sciences, Faculty of Pharmacy, Department of Pharmaceutical Technology, Uskudar, 34668 İstanbul, Turkey.

E-mail address: neslihanustundag@yahoo.com (N. Üstündağ Okur).

Peer review under responsibility of King Saud University.



Production and hosting by Elsevier

when an infection has developed (Dai et al., 2010). Election of topical antimicrobial therapy should be based on the agent's ability to inhibit the microorganisms recovered from burn wound surveillance cultures (Altöparlak et al., 2004). Fusidic acid (FA) is an antibiotic agent derived from the fungus *Fusidium coccineum* (Lee et al., 2015), belongs to the class of steroids, but has no corticosteroid (anti-inflammatory or immunosuppressive properties) effects. Nowadays, it is available in many formulations for oral (tablet and suspension), intravenous, and topical (cream and ointment) administration. For skin infections treatments, many doctors prescribe topical fusidic acid. The most frequent indications are boils, anthrax or carbuncle, erythema, cellulitis, folliculitis, acne, paronychia, hidradenitis, and wound infections due to burns and impetigo (Banerjee and Argaez, 2017; Bonamonte et al., 2014).

A microemulsion is defined as a dispersion consisting of oil, surfactant, co-surfactant and aqueous phase, which is a thermodynamically stable liquid solution. They are homogenous dispersions of water in oil (w/o) or oil in water (o/w) droplets stabilized by surfactants (Hamed et al., 2019; Üstündağ Okur et al., 2011). From preparation and sterilization, microemulsions are relatively simple and inexpensive systems (Kaur et al., 2018). These formulations are also used to prepare poorly water-soluble drugs because their structure allows the solubilization of lipophilic drugs in the oil phase (Üstündağ-Okur et al., 2014a). The administration of microemulsions as a solution onto the skin can be challenging due to its low viscosity. To optimize the microemulsion as a dermal formulation, different hydrogels such as chitosan, xanthan gum, carbomer, and carrageenan have been studied to increase the viscosity of formulations (Ghorbanzadeh et al., 2019). To minimize this effect the thickening agent can be introduced into the system in order to transform it from liquid to semisolid state (Froelich et al., 2019). The addition of gelling components into microemulsions produces microemulsion-based hydrogels, which are easier to apply to the skin compared to runny liquid formulations (Hajjar et al., 2018). The stable microemulsion based hydrogel has good permeation ability and suitable viscosity for the topical delivery, which provided longer contact with skin (Ghorbanzadeh et al., 2019).

The aim of this work was to develop novel FA loaded microemulsion formulations for burn healing treatment. For this purpose, characterization, drug release, stability, anti-inflammatory activity and *in vivo* of the formulations were investigated.

2. Materials and methods

2.1. Materials

FA was a kind gift from Berko İlaç, Turkey. Ethyl oleate (EO) was purchased from Sigma-Aldrich, UK. Chitosan oligosaccharide lactate (COL) was obtained from Sigma-Aldrich, USA. Tween 80 (Polysorbate 80) and Nutrient Agar (1.05450) were purchased from Merck, Germany. Acetonitrile (Sigma, Germany) was used for high pressure liquid chromatography (HPLC). Ultrapure water was obtained from Direct-Q® Water Purification System, Germany. Spectra/por dialysis membrane was purchased from Spectrum. Fluid Thioglycollate Medium (CM0173) and Soy Bean Casein Medium were obtained from Oxoid, Thermo-Fisher Scientific. Mueller-Hinton II Agar (70191) was purchased from Sigma-Aldrich Co. Type cultures of bacteria were purchased from ATCC, USA. Dulbecco's modified Eagle's medium (DMEM) was obtained from Gibco, USA, MTT was purchased from AppliChem, Germany. Isopropanol, sulfanilamide and N-(1-naphthyl)ethylenediamine dihydrochloride were purchased from Sigma-Aldrich, USA, phosphoric acid from Mettler, Switzerland.

2.2. Preparation of microemulsion formulation

The existence range of microemulsions was understood by using pseudo-ternary phase diagrams. Titration method was used to obtain microemulsions. A series of oil and surfactant/co-surfactant mixtures (1:1, 2:1, 3:1, 4:1, 5:1, 6:1, 7:1, 8:1, and 9:1 at weight ratios) with ultrapure water at 25 ± 1 °C were titrated. After that, microemulsions were determined by visually examining the mixtures. The HLB value of formulation was determined as 15. A software program was used to construct the phase diagrams. All preparations were repeated at least four times. Microemulsion formulation was developed in accordance with the microemulsion area in the phase diagrams. After gently equilibrating, selected microemulsions for 5 min were magnetic stirred. To check physical stability for ideal microemulsion, fresh and aged microemulsion formulations were tested by applying centrifugation test. The microemulsions were subjected to centrifugation at 5.175g for 30 min and observed for any phase separation (Üstündağ-Okur et al., 2014b; Üstündağ Okur et al., 2016).

2.3. Preparation of FA loaded microemulsion based gel

In Table 1, the list of the materials that were used for preparing formulations in the present work, together with their abbreviations is provided. For preparing microemulsion based gel (MBG) COL (1%) was added to the water phase of the microemulsion.

2.4. Characterization of formulations

In order to detect the suitability of formulations for topical administration, formulations were evaluated for their characteristic features such as pH, viscosity, droplet size, polydispersity index (PDI), zeta potential, drug content and spreadability.

2.4.1. Droplet size, PDI and zeta potential analysis

Dynamic Light Scattering method (Nano ZS, Malvern Instruments, U.K.) was used to measure the average droplet size and PDI. Experiments were repeated six times at 25 ± 1 °C. In order to measure the zeta potential of samples, capillary zeta cells were used. By using the Helmholtz-Smoluchowski equation, the zeta potential was detected. Software involved system was used for the process. The experiments were repeated six times at 25 ± 1 °C (Üstündağ-Okur et al., 2014a).

2.4.2. Viscosity

Brookfield viscometer LVDV-E model was used to determine the viscosity of the formulations. The preparations were placed in the sampler tube. The formulations were measured with 50 rpm at 25 ± 0.5 °C.

2.4.3. Determination of pH

The pH of the formulations was detected using a calibrated pH meter (Mettler Toledo, Switzerland). Determinations were carried out four times.

Table 1

Components concentration (%) of the prepared microemulsion (M) and microemulsion-based gel formulations (MBG).

Component (%)	M	MBG
EO	14.58	14.58
Tween 80	53.75	53.75
EtOH	8.958	8.958
Water	22.71	22.71 (1% COL)
Surfactant/Cosurfactant ratio	6:1	6:1

2.4.4. Drug content

To determine drug content in the prepared formulations, the drug loaded formulations were dissolved in methanol and investigated with HPLC.

2.4.4.1. HPLC studies. The mobile phase was prepared by mixing acetonitrile and ultrapure water (80:20) (v/v) with a flow rate of 1.7 mL/min. The flow rate was 1.7 mL/min and the column temperature was maintained at 25 ± 1 °C at 285 nm. The volume of injection was adjusted 20 μ L. The run time was set at 10 min with the system operating at 25 ± 1 °C. The HPLC method was validated for linearity, the limit of detection and quantitation, precision, accuracy and specificity, selectivity and stability (Üstündağ Okur et al., 2016).

2.4.5. Spreadability

To determine spreadability of formulations, 100 mg of blank and FA loaded formulations were transferred to the center of a glass plate at 32 °C. This plate was compressed under another plate. After one minute, the weight was removed and the diameter of the spread area (cm) was measured.

2.4.6. Stability of FA loaded microemulsion based gel

In physical stability studies, the formulation (FA-MBG) was placed at 4 ± 0.5 °C in the refrigerator and 25 ± 1 °C (relative humidity 60%) in the stability cabinets (Nuve, Turkey) for three months. After three months; visual appearance, clarity, pH, spreadability of the gel and FA content were determined.

2.5. In vitro drug release studies

In vitro release experiment of microemulsion based gel formulation was performed in ethanol and PBS pH 7.4 (ratio of 30:70) at 50 rpm at 32 ± 0.5 °C. 5000 mg of FA-MBG was separated from release media by means of dialysis membrane (Spectra/por, MW of 12–14 kDa). 1 mL of sample was withdrawn at a predetermined time interval of 0.5, 1, 2, 3, 4, 5, 6, 7, 8, 10, 12 and 24 h. The samples were analyzed with HPLC. The experiment was repeated three times.

2.6. Microbiological studies of FA loaded microemulsion based gel

2.6.1. Sterility studies

FA loaded MBG were prepared at Laminar air flow Cabinet (Haier HR40-IIA2). Sterility testing of the formulation was carried out under aseptic conditions. To check the sterility of the blank and FA loaded MBG sterility control testing was performed according to the international Pharmacopoeia (*The International Pharmacopoeia Fourth Edition*) and similar to the previously reported method (Üstündağ Okur et al., 2019b). For anaerobic bacteria, the Fluid thioglycollate medium was used. 1 mL of the formulation was added to each medium and incubated in BINDER GmbH incubator at 35 °C for bacteria and 25 °C for fungi for two weeks. No growth of the microorganisms occurred. For growth promotion test of aerobes, anaerobes and fungi, fluid thioglycollate media (using a separate portion of media for each microorganism) were inoculated with 100 CFU of *Staphylococcus aureus* ATCC 6538, *Clostridium sporogenes* ATCC 19404 and *Candida albicans* ATCC 10231. Media were incubated at 35 °C for 48 h.

2.6.2. Disk diffusion testing

The antibacterial effect of the microemulsion based gels both with FA and without FA and the commercial product (Fucidin 2%, Abdi İbrahim) was tested on *S. aureus* (ATCC 6538), *Bacillus cereus* (ATCC 7064), *Escherichia coli* (ATCC 8739), *Pseudomonas aeruginosa*

(ATCC 27853), using both agar well diffusion method according to the guidelines of Clinical and Laboratory Standards Institute (standard M02-A) and previously reported methods (Siafaka et al., 2019). Staphylococci are known to induce skin abscesses and worldwide they are the most commonly identified agent responsible for skin and soft tissue infections (Kaplan et al., 2005; Siafaka et al., 2016; Üstündağ Okur et al., 2019a). Gram negative *P. aeruginosa* is also known to be a common and increasing reason of skin infections that can result in potentially life-threatening septicemia (Siafaka et al., 2016; Siebenhaar et al., 2007).

Bacteria were incubated on Nutrient Agar at 37 °C for 18 h. Active cultures were aseptically suspended in sterile saline and were arranged to give an inoculum with an equivalent cell density to 0.5 McFarland turbidity standard. 100 μ L of each sample was spread evenly onto Mueller-Hinton II Agar and allowed to dry, and wells (diameter = 10 mm) were filled with 100 μ L of formulations. They were stored at 37 ± 1 °C for 24–48 h and the inhibition diameters of each formulation for each isolate were detected by a digital ruler. Each test was completed in triplicate and the mean zone size was detected.

2.7. Anti-inflammatory activity

2.7.1. Cell culture

The murine macrophage cell line RAW 264.7 was obtained from American Type Culture Collection, USA (ATCC). Cells were cultured in Dulbecco's modified Eagle's medium (DMEM, Gibco, NY, USA) supplemented with 10% heat-inactivated FBS and 1% penicillin (10,000 units/mL) and streptomycin (10,000 μ g/mL) in a humidified atmosphere of 5% CO₂ at 37 °C. The effect of MBG and FA-MBG on cell viability, MTT colorimetric assay was used. Briefly, RAW 264.7 cells were plated at a density of 1×10^6 /mL and incubated for 24 h at 37 °C in 5% CO₂. After 24 h, cells were treated with MBG and FA-MBG (0.025%, 0.05%, 0.1%, 0.2%). After 24 h of incubation, the cell culture medium was discarded and MTT solution (0.5 mg/mL) was added to each well for an additional 2 h at 37 °C. After 2 h incubation, the cell culture medium was discarded and 100 μ L of isopropanol was added to wells to dissolve formazan crystals. The optical density was measured at 570 nm wavelengths using an ELISA microplate reader (Thermo Multiskan Spectrum, Finland) (Reis et al., 2018). The percentage of cell viability was detected by using the following equation:

$$\text{Viability}\% = (\text{Absorbance}_{\text{treatment group}}) / (\text{Absorbance}_{\text{control}}) \times 100\%.$$

2.7.2. Evaluation of anti-inflammatory activity by Griess assay

To determine the anti-inflammatory activity of the MBG and FA-MBG on RAW 264.7 cells, the Griess assay was performed (Reis et al., 2018). Briefly, RAW 264.7 cells plated in a 48 well-plate at a density of 1×10^6 /mL and incubated for 24 h at 37 °C in 5% CO₂. After 24 h of incubation, plated cells were pre-treated with MBG and FA-MBG (0.025%, 0.05%, 0.1%, 0.2%) for 2 h and then stimulated with 1 μ g/mL of LPS (lipopolysaccharide from *Escherichia coli* 0111:B4, Sigma, USA) for additional 22 h. After total 24 h, 50 μ L of cell culture supernatant was mixed with 50 μ L Griess reagent in a 96-well plate (1% sulfanilamide and 0.1% N-(1-naphthyl) ethylenediamine dihydrochloride in 5% phosphoric acid) for 10 min in the dark at room temperature. The optical density was measured by using a microplate reader (Multiskan Ascent, Finland) at 540 nm wavelengths. The nitrite levels were determined by using sodium nitrite standard calibration curve. Indomethacin (100 μ M) was used as a positive control.

2.7.3. Statistical analysis

All repeated experiments were conducted in triplicate. Statistical analysis of the results was performed by using GraphPad Prism

6 (Version 6.01; GraphPad Software, Inc., San Diego, CA). Differences between groups were analyzed by using one-way ANOVA following the post-hoc tests by Tukey. Group differences were considered to be significant at $p < 0.05$ (*), $p < 0.01$ (**), $p < 0.001$ (***)

2.8. In vivo studies

2.8.1. Animals

All animal studies were performed according to the Declaration of Helsinki and approved by the Local Animal Ethical Committee (Approval number: 38828770-604.01.01-E.46499). Male Wistar albino rats weighing 250 ± 10 g were purchased from the Experimental Animal Center of Istanbul Medipol University for the animal experiment. Rats were housed in a room maintained at 22 ± 1 °C with an alternating 12-h light/dark cycle. Animals had free access to a pellet diet and water ad libitum. The rats were transported to a quiet laboratory at least 1 h before the experiment began. For the *in vivo* studies, all studies were done between 09:00 to 12:00 a.m. under the normal room light and temperature (22 ± 1 °C).

2.8.2. Experimental groups and burn model

21 animals were divided into 3 groups ($n = 7$) each as follows;

- (1) Control group (Untreated group): CG
- (2) Fusidic acid (2%) loaded microemulsion based (FA-MBG) gel group: MG
- (3) Fucidin® (2% Fusidic acid) cream group (commercial product of FA): RG

All rats were anesthetized with ketamine (10 mg/kg)-xylazine (80 mg/kg) and the back of each animal was depilated and washed with the solution of povidone-iodine. The 2nd degree burn wounds (two full-thickness burn wounds per rat) were induced on the surgical area by using a temperature controlled modified heating instrument. The heated template (1 cm diameter) was applied perpendicularly to the designated area with gravitational pressure and temperature of 100 °C for 15 s (Oryan et al., 2018). The standard drug and the formulations (0.5 g) were topically applied once a day for 10 days.

2.8.3. Burned wound area measurement

Each burned wound site pictures were obtained with a camera (Canon, Japan) at days 0, 3, 5, 7, and 10 to measure wound contraction. The wounds photographs were performed at a 90° angle. An image analyser (Image J.2.0 software, NIH, USA) was used to detect wound surface areas during healing. The wound closure % was detected as follows:

$$\% \text{ Wound contraction} = (\text{Current wound area/wound area at the beginning}) \times 100 \text{ (Okur et al., 2018).}$$

2.8.4. Histology

The animals were sacrificed and the wound tissues were removed on day 10. The samples were fixed in 10% formalin, for one day and then embedded in paraffin, sever to 5 µm-thick portions, and dyed with Hematoxylin & Eosine for scoring under light microscopy. The histologic score system ranged between 1 and 4. Wound healing for each group was evaluated using the scoring system for epidermal and dermal regeneration described by Galeano et al. (2006), (Ayla et al., 2017).

2.8.5. Statistical analysis

GraphPad Prism 7.0 was used for statistical analyses and graphs. The results were expressed as means \pm standard error of the mean (SEM). Significant differences between groups were

determined by one-way ANOVA using a Kruskal–Wallis test. Values for $p < 0.05$ were considered statistically significant.

3. Results and discussion

A burn is a common medico-surgical problem all over the world. It is probably the most devastating of all wounds (Dua et al., 2013). The imbalance between the pathological factors and integrity of immune defense mechanism promotes colonization of both gram-positive and gram-negative bacteria on the burning surface including *P. aeruginosa*, *S. aureus* and Methicillin-resistant *S. aureus* (Serra et al., 2015; Üstündağ Okur et al., 2019a). Owing to the high amount of antimicrobial on the lesion surface, ease of rapid delivery, better adherence and decreased systemic toxicity risk, topical-antimicrobial therapy has always been considered advantageous (Lipsky and Hoey, 2009). However, creams and ointments fail to remain adhered to the lesion site and lose their rheological properties as they come in contact with the lesion fluid. This brings impaired drug delivery and increased applications of antibiotic (Thakur et al., 2018).

FA is the only fusidane-type antibiotic that has been clinically used. It has been applied to treat infections caused by methicillin resistant *Staphylococcus aureus* strains, and it is also effective against other species of Gram-positive bacteria FA blocks the translation elongation factor G gene in bacteria. Translation EF-G interacts consecutively with the ribosome during polypeptide synthesis (Salama et al., 2013). The conventional topical formulations of FA fail to penetrate across the wound eschar leading to sub-optimal therapeutic efficacy and moreover, it has to be applied 2–3 times daily (Schöfer and Simonsen, 2010).

In addition, some anti-bacterial agents (the nephro/hepatotoxicity of silver, argyria and dyschromia) for burned wounds, are not so advantageous as it is believed. Moreover, conventional wound dressings have several limitations including adherence to wound, resulting in ischemia and/or necrosis, the occurrence of a foreign-body reaction, and irritation, or allergic reaction (Oryan et al., 2018). Thus, the development of novel dressings with significant properties is mandatory.

3.1. Preparation and characterization of FA loaded microemulsion based gel

Fig. 1 shows pseudo-ternary phase diagram of microemulsion composed of EO, tween 80, ethanol and distilled water. The construction of phase diagrams was used to detect the concentration range of components in the presence of microemulsion. The blank microemulsion was selected from the gravity center of the phase diagram. The surfactant/co-surfactant ratio with the highest area was determined as 6:1. The area of M1 microemulsion was determined as 862.04. It should be claimed that this phase diagram was obtained by maintaining the surfactant/co-surfactant ratio at 6:1. Hydrophilic lipophilic balance (HLB) value was determined as 12.077. After FA was dissolved in the system, the clear system was detected with no phase separation. The microemulsions had isotropic transparent dispersions and after centrifugation, no phase separation was observed. This demonstrated the good physical stability of the tested microemulsions.

Nonionic surfactants are known to be less toxic than ionic surfactants. In this study, tween 80 was used as a nonionic surfactant. Surfactants with high HLB (>12) values assist the immediate formation of o/w droplet and rapid spreading of the formation in aqueous media (Solans and García-Celma, 1997). Ethanol was applied as cosurfactant. Short to medium chain length alcohols are generally added as co-surfactants to increase the fluidity of interface (Szumala, 2015).

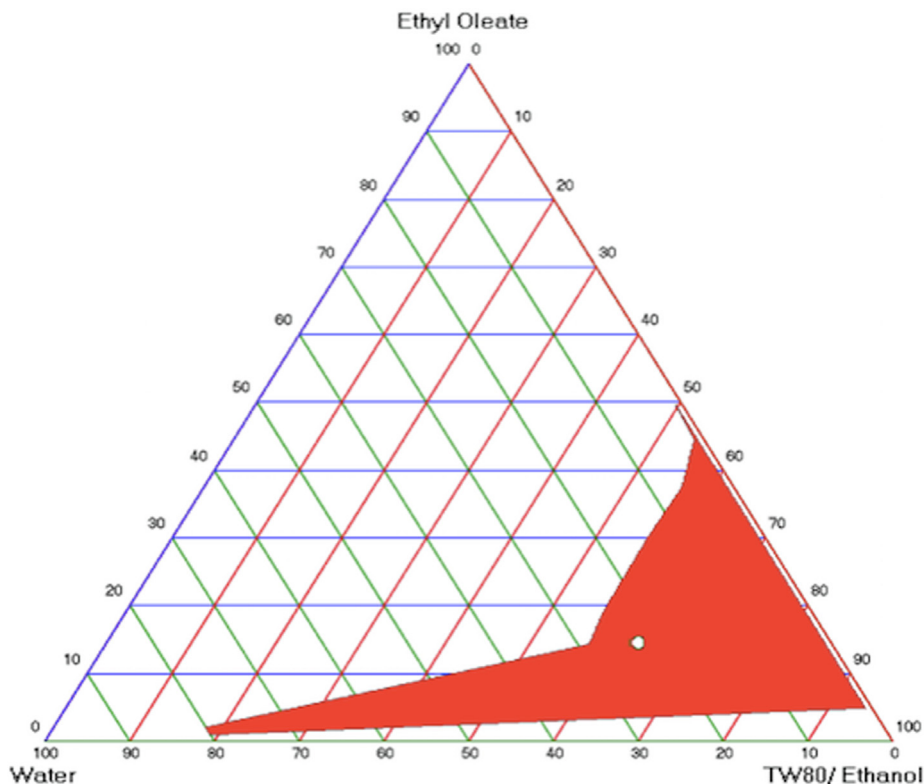


Fig. 1. Pseudo-ternary phase diagrams of microemulsion composed of EO, Tween 80: Ethanol ratio 6:1 and distilled water.

Microemulsion-based gel was successfully prepared with COL (1%) as a gelling agent to impart viscosity to the preparation as well as to sustain the action of the drug by increasing residence time. Polysaccharides have been considered to encourage wound healing which is quite important for the development of effective and non-toxic drugs with better activities *in vitro* and *in vivo* (Trabelsi et al., 2017).

Physicochemical characterization of microemulsion formulations especially for dermal application is an important subject to be considered during the formulation development phase (Üstündağ Okur et al., 2011). The physicochemical characterization parameters of blank microemulsion (M), FA loaded microemulsion (FA-M), blank microemulsion based gel (MBG) and FA loaded microemulsion based gel (FA-MBG) is reported in Table 2. The droplet size of M and FA-M ranged from 9.39 to 11.22 nm with low PDI values. On the other hand, the droplet size of MBG and FA-MBG ranged from 20.56 to 21.27 nm with low PDI values. It can be said that FA entrapment increased the droplet size. Similar results have been reported for rosiglitazone-loaded cationic lipid emulsion (Davaa and Park, 2012). A near-neutral surface charge was observed for M and FA-M formulations. Zeta potential of MBG and FA-MBG was found as 15.8 ± 1.03 and 14.69 ± 0.92 mV, respectively. Spreadability test was carried out for all the formulations since it is important for patient compliance and helps in the uniform application of gel to the skin

(Shishoo et al., 2011). Spreadability values of the MBG and FA-MBG were decreased compared to microemulsion spreadability which could be associated with COL addition. The pH values of formulations ranged from 5 to 5.41, are close to the pH values of normal skin. This fact can imply formulations compatibility with skin. The viscosity of MBG was significantly higher than that of M (1523.33 ± 2 cP vs 692.53 ± 1.25 cP). It can be claimed that the increase of viscosity was due to the addition of COL, since gelling agents such as chitosan can increase the viscosity of formulations. This enhanced viscosity improves the suitability of formulations for topical administration (Üstündağ Okur et al., 2019b). Finally, the drug content uniformity of FA-M and FA-MBG was found to be 95.42 ± 3.07 , 95.36 ± 4.15 , respectively. Similar drug content results also revealed by Mali et al., where microemulsions loaded with lipophilic itraconazole were studied (Mali et al., 2017). Besides, microemulsions and microemulsions based gels are chosen for topical administration systems due to their enhanced drug entrapment and their ability to solubilize the lipophilic drug moiety which shows rapid and efficient penetration to the skin (Mehta et al., 2015).

Due to the above characterization results, as optimal dermal carrier was chosen FA-MBG and thus it was further studied in context of stability and *in vitro* release. In later stages, antimicrobial activity and healing properties were also evaluated for the chosen desirable carrier.

Table 2
Characterization results of blank and FA loaded microemulsion and microemulsion based gel formulations.

Formulation code	pH	Viscosity (cP)	Droplet size (nm)	PDI	Zeta potential	Spreadability (cm)	Drug content (%)
M	5 ± 0.06	692.53 ± 1.25	11.22 ± 0.22	0.45 ± 0.08	-1.45 ± 0.36	4.5 ± 0.05	–
MBG	5.41 ± 0.05	1523.33 ± 2	20.56 ± 0.37	0.312 ± 0.01	15.8 ± 1.03	3.28 ± 0.18	–
FA-M	5.04 ± 0.02	410.43 ± 0.75	9.39 ± 0.29	0.47 ± 0.1	-1.05 ± 0.54	5.35 ± 0.30	95.42 ± 3.07
FA-MBG	5.07 ± 0.02	1468.33 ± 2.7	21.27 ± 0.195	0.308 ± 0.03	14.69 ± 0.92	3.07 ± 0.12	95.36 ± 4.15

3.2. Stability studies of FA loaded microemulsion based gel

The stability experiments were performed at 4 ± 1 °C and 25 ± 1 °C, for a period of 3 months. Table 3 shows stability studies results of FA-MBG formulation. There was no significant change in clarity, pH and drug content of the FA-MBG after 3 months of stability testing. Thus, the prepared FA-MBG can be declared as stable at 4 °C and room temperature for 3 months.

3.3. In vitro drug release study of FA loaded microemulsion based gel

In vitro drug release of the microemulsion was evaluated via dialysis bag technique, using pH 7.4 as release medium. Fig. 2 depicts *in vitro* drug release results of FA-MBG. It is well reported that FA is not soluble in water, so a very low dissolution rate has been reported in pH = 7.4. First of all, it can be indicated that prolonged- controlled release pattern with 10% burst effect was achieved. Nonetheless, improved gradual release of FA for 24 h is seen. Finally, maximum drug release from microemulsion based gel was achieved within 24 h. Similarly, numerous studies can be found which exhibit that lipophilic drug loaded microemulsions showed prolonged release (Froelich et al., 2017; Olejnik et al., 2018; Ustündağ Okur et al., 2014).

3.4. Microbiological studies of FA loaded microemulsion based gel

Wound infection is a big problem in burn therapy since it is the most prevalent reason of mortality (D'Avignon et al., 2010; Merchant et al., 2015; Norbury et al., 2016). Pathogens have evolved over time in line with antibiotic use (Wang et al., 2018). With limited new antibiotics, discoveries increasing the efficacy of currently available antimicrobials is remarkable to enhance morbidity in burn sufferer (Kinch et al., 2014). Infection not only could have serious threats on patient's life, but it also delays the healing process resulting in prolonged hospitalization time and cost (Oryan et al., 2018; Sifaka et al., 2016). Burns are particularly susceptible to infection for several reasons. The disruption of the epidermal barrier combined with the denaturation of proteins and lipids provides a fertile environment for microbial growth (Sevgi et al., 2013). From the results of the sterility studies of the formulations with FA, it was demonstrated that no growth of any of the inoculated microorganisms occurred after the incubation period. Moreover, it can be reported that the prepared microemulsion based gel showed an antibacterial effect on the selected microorganisms. Fig. 3 shows zone inhibition diameters of FA-MBG, MBG and commercial product of FA. Blank MBG (not containing FA) as it was expected did not show any inhibition zones on *E. coli* and *P. aeruginosa*, which are both gram negative bacteria. In gram positive bacteria (*S. aureus* and *B. cereus*) there was a minor inhibition zone, probably due to COL addition. It is well known, that chitosan possesses antimicrobial activity against some strains (Sifaka et al., 2016). The microemulsion based hydrogel showed greater inhibition zone diameters for all the bacteria except *P. aeruginosa* compared to the commercial product (Table 4). According to our results, while *P. aeruginosa* and *E. coli* showed the nar-

rowest inhibition zone, the largest zone was observed in *S. aureus*, which is the most reported bacterium that causes infections on soft tissues.

3.5. Anti-inflammatory activity

Before analyzing the potential anti-inflammatory activity of the MBG and FA-MBG by measuring nitrite levels in cell culture medium, non-toxic concentrations with viability more than 70% were determined. Therefore, cytotoxic effects of MBG and FA-MBG were examined on RAW 264.7 murine macrophage cells by MTT colorimetric assay after 24 h of treatment with varying concentrations (0.025%, 0.05%, 0.1%, 0.2%) of MBG and FA-MBG. Fig. 4 shows effect of MBG and FA-MBG on RAW 264.7 cell viability. It can be concluded that viability is high and acceptable for such formulations. These results are rational given that the used chemical substances are non-toxic.

3.5.1. Nitric oxide production in Lps-stimulated RAW 264.7 cells

Nitric oxide (NO) is well known to be one of the major regulators of wound healing. However, excessive NO production was demonstrated to play a critical role in the pathogenesis of inflammation and can lead to cellular death and tissue damage in high amounts by reacting with reactive oxygen species (Schulz and Stechmiller, 2006). Therefore, inhibition of NO production is an important strategy for the screening of anti-inflammatory formulation.

In the present study, both of the formulations, MBG and FA-MBG exert anti-inflammatory effects in LPS induced RAW 264.7 macrophage dose dependent manner. The effects of MBG and FA-MBG on NO production were assessed by Griess assay by evaluating the decrease in nitrite production levels *in vitro*. As in Fig. 5, MBG and FA-MBG decreased nitrite levels by up to 80% in LPS-stimulated RAW 264.7 cells and showed the strongest anti-inflammatory affect at the highest dose administered (0.2%).

3.6. In vivo studies

3.6.1. Macroscopic burn healing

In this study, the burn healing potential was evaluated through 10 days experimental period by monitoring regularly the percentage of wound areas contraction. Experimental 2nd degree burns were created on the backs of rats and all lesions were treated for 10 days to investigate the burn healing activity of FA loaded microemulsion based gel group (MG). The degree of a burn injury can be classified into first, second, third, or fourth degree burns according to the depth of tissue injury. 2nd degree burns can affect either papillary layer (i.e. the upper dermis) or reticular layer (i.e. the deeper dermis) with white or yellow color, blistering of the skin, and a moist appearance (Mofazzal Jahromi et al., 2018).

The daily behaviors (food intake, activity, e.g.) of rats were observed as normal. The macroscopic photos of the burn areas on days 0, 3, 5, 7 and 10 were presented in Fig. 6. On day 1, necrosis and edema were observed on the wound surface areas in all groups. Exudates were also seen, and the edges of the wounds started to pronounce. Edema was also present around the wound surface area. Crust formations were observed on the skin after several days. It was found out that MG treatment did not get irritated the skin. Furthermore, on the 10th day, the crust layer of MG was fell off.

The wound contraction ratio was assessed as the percentage reducing in wound size on days 0, 3, 5, 7, and 10. As it is illustrated in Fig. 7, MG showed a significant burn healing progression on the day 3 ($P < 0.01$), 5 ($P < 0.01$), 7 ($P < 0.01$), and 10 ($P < 0.01$) compared to untreated group. The healing percent of lesion area ranged

Table 3
Stability studies of FA-MBG formulation.

Parameters	t = 0 months	t = 3 months	
	4 ± 0.5 °C/ 25 ± 1 °C	4 ± 0.5 °C	25 ± 1 °C
pH	4.47 ± 0.02	5.117 ± 0.012	5.053 ± 0.015
Spreadability (cm)	3.07 ± 0.12	1.850 ± 0.071	1.875 ± 0.035
Drug content (%)	95.36 ± 4.15	95.070 ± 2.445	94.053 ± 1.477

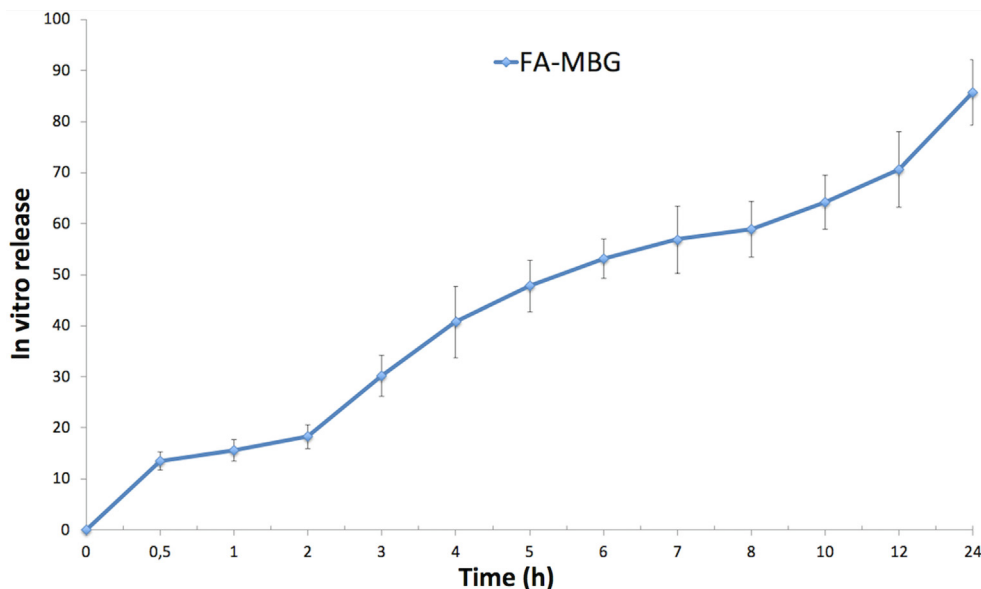


Fig. 2. In vitro drug release results of FA-MBG (n:3, \pm STD).

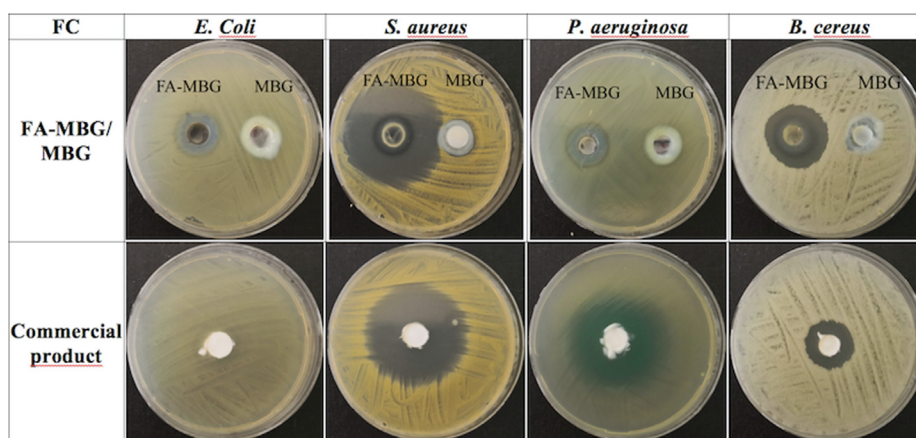


Fig. 3. Zone inhibition diameters of FA-MBG, MBG and commercial product of FA.

Table 4

Microbiological studies results of formulations with FA (FA-MBG), without FA (MBG) and commercial product of FA.

	FA-MBG (mm)	MBG (mm)	Commercial product (mm)
<i>E. coli</i>	17–17	0–0	10–9
<i>S. aureus</i>	50–51	19–18	47–49
<i>P. aeruginosa</i>	20–20	0–0	40–40.5
<i>B. cereus</i>	30–29	16–16	24–24

from 90.11% to 65.49% in the period from 3 to 10 days in the control group (CG). The % of the burn area treated with RG ranged from 77.29% to 46.71% in the period from 3 to 10 days. The % of wound area in rats treated with MG ranged from 69.30% to 41.39% in the period from 3 to 10 days. Compared to the control group, MG and RG recovered quickly and the burn area rapidly decreased in size by the tenth day. The main objective in burn injury healing is the early wound closure and rapid replacement of normal skin with minimal scarring (Kaita et al., 2019; Mofazzal Jahromi et al., 2018).

3.6.2. Histology of wound healing

Histopathological analysis showed differences in the healing phase of the control group and the groups. Wound healing is a complex and continuous process, but for descriptive purposes, it is divided into 3 biologically distinct, although overlapping stages; the inflammatory, the repair or proliferative, and the remodeling stage (Okur et al., 2018). Extensive tissue damaged during burns impairs angiogenesis, collagen re-organization, granulation tissue formation and induces free radical-mediated damage which results in delayed tissue repair (Heidari et al., 2019). From the 3rd day, a proliferative phase has been triggered and characterized by the formation of granulation tissue, including angiogenesis, the migration of fibroblasts, and collagen synthesis (Sellimi et al., 2018).

The microscopic photos were taken during the histological examination of the wound tissues on the 10th day are given in Fig. 8. Histopathological examination of wound tissues on the 10th day is illustrated in Fig. 9.

In the present study, hematoxylin and eosin stained sections of wound tissues were used to evaluate re-epithelization, revascularization and organization of granulation tissue.

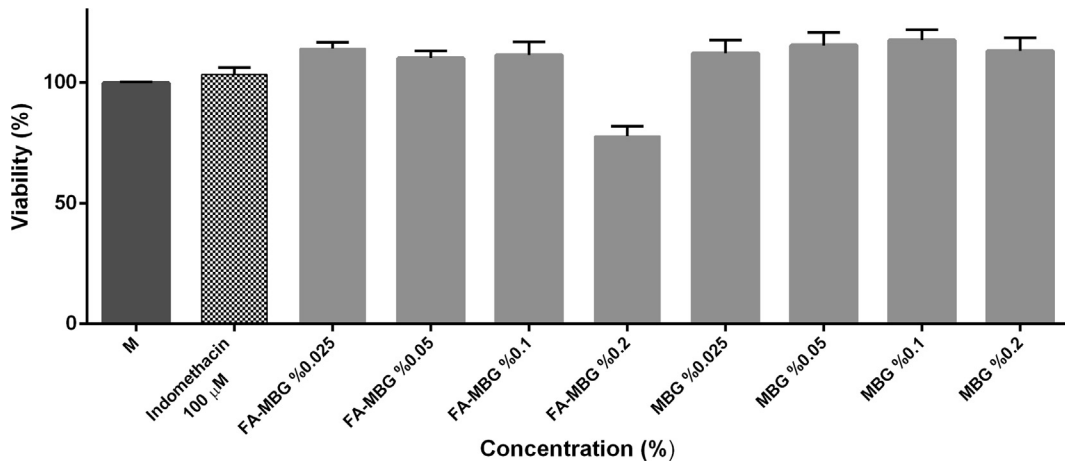


Fig. 4. Effects of MBG and FA-MBG (0.025%, 0.05%, 0.1%, 0.2%) on RAW 264.7 cell viability. Cells were treated with indicated concentrations of MBG and FA-MBG for 24 h and then cell viability was assessed by MTT assay. Untreated cells taken as 100% viability.

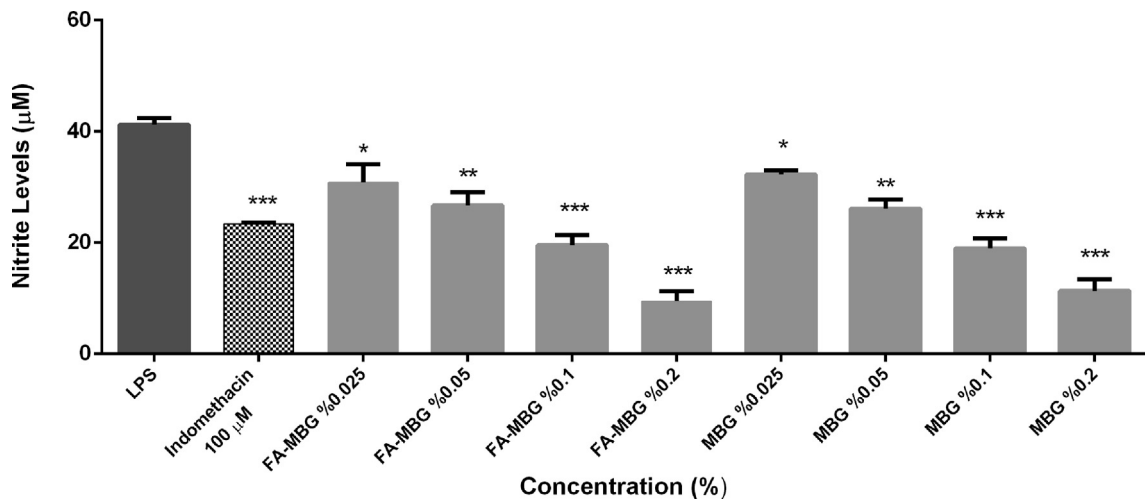


Fig.5. Effects of MBG and FA-MBG (0.025%, 0.05%, 0.1%, 0.2%) on the nitrite production in 1 µg/ml LPS-induced RAW 264.7 cells.

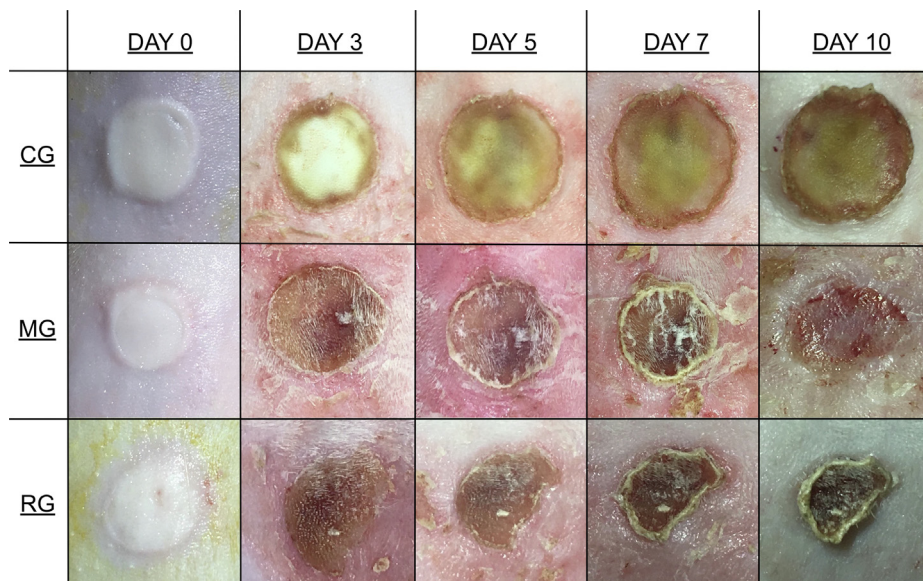


Fig. 6. Effects of MG on wound's evolution. Macroscopic examples of wound healing with control (CG), MG, and Fucidin® (RG) groups after excision on days 0, 3, 5, 7, and 10.

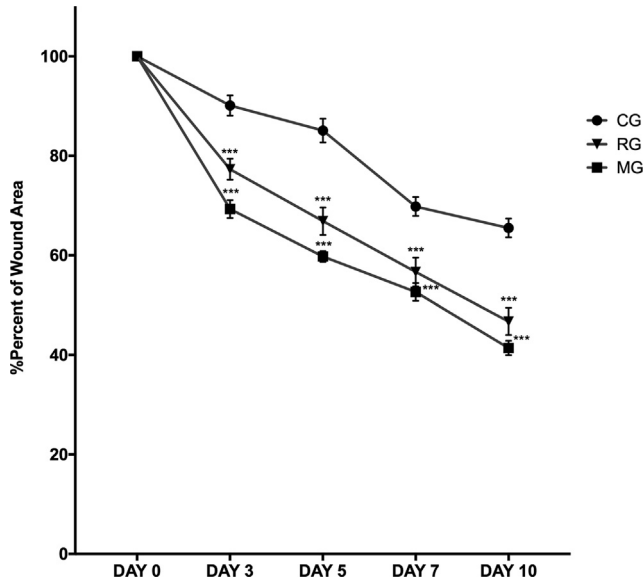


Fig. 7. The rate of wound healing of scar tissue surface area in animal groups on days 0–10. Each data point represents the mean ± SEM.

As stated in the obtained outcomes, it was determined that MG and RG had a significant effect compared to the control group (Figs. 8–9).

It has been shown that there were significantly higher percentages of dermal and epidermal regeneration with the MG ($P < 0.05$) and RG ($P < 0.05$) in comparison to the untreated group (Figs. 8–9). Re-epithelialization is induced by activation of cytokines and growth factors which cause expansion of keratinocytes, epithelial cells, stem cells and fibroblasts (Mofazzal Jahromi et al., 2018).

According to the histological evaluation results, more blood vessel formation was detected on MG ($P < 0.05$) and RG ($P < 0.05$) in comparison to the untreated group. Angiogenesis phase, several growth factors and thrombin, which are the foremost activating molecules for endothelial cell growth (Mofazzal Jahromi et al., 2018).

Moreover, it was seen that thicker granulation tissue was formed in the MG ($P < 0.01$) in comparison to the untreated group after treatment (Figs. 8–9). Also, MG provides new granulation tissue formation more than RG ($P < 0.05$) (Figs. 8–9). The final step of the proliferation phase is the production of granulation tissue, which can be specified by the presence of many fibroblasts, granulocytes and macrophages (Mofazzal Jahromi et al., 2018).

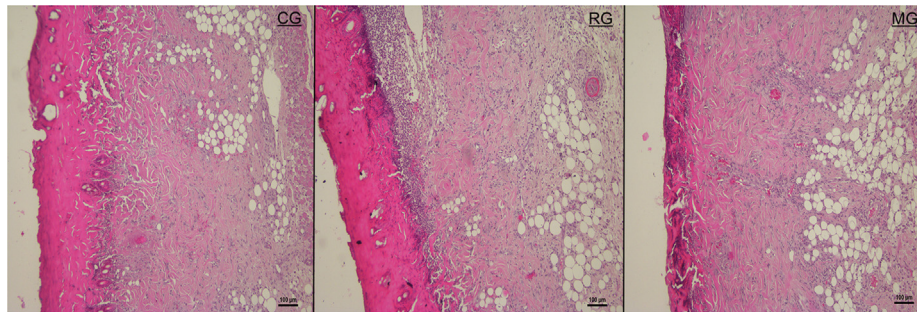


Fig. 8. Histopathological view of scarred tissues of the control (CG), FA (2%) loaded MBG gel (MG), and Fucidin® (RG) groups on the 10th day after the burning process (Hematoxylin and eosin (H&E) (original magnificationX10). The scale bars represent 100 µm for the figure.

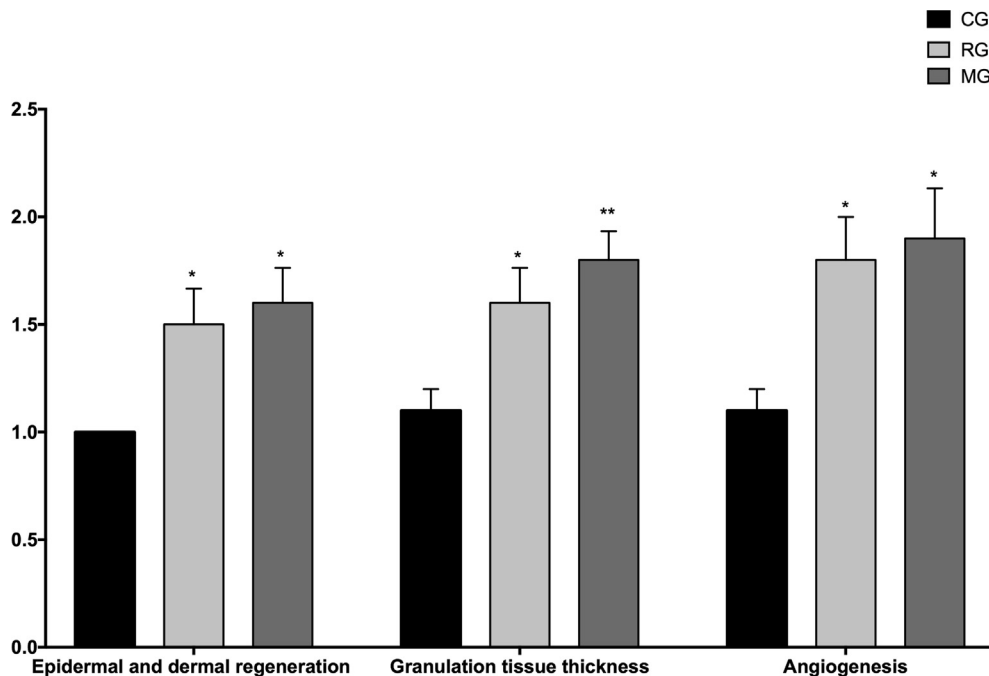


Fig. 9. Microscopic investigation of granulation tissue thickness, angiogenesis and epidermal-dermal regeneration on control (CG), FA (2%) loaded MBG gel (MG), and Fucidin® (RG) groups by histological wound healing scores among. Statistically significant as compared to control; $P < 0.05$ (*), $P < 0.01$ (**).

4. Conclusion

In this work, the potential of FA loaded MBG as drug carriers for dermal delivery was evaluated. The findings indicated that MBG formulation exhibited significant antibacterial properties. This result provided support for the promising use of FA for applications as a therapeutic agent for dermal wound healing. The developed system demonstrated improved wound healing, good spreadability and enhanced therapeutic efficacy given that at the end of the 10th day of *in vivo* experiment, the healing percent of lesion area was found as 46.71% for commercial product and 41.39% for FA-MBG. In conclusion, the present study can open up a window for dermal application of MBG loaded with FA, and it would be a better alternative to conventional dermal creams in burn healing.

Declaration of Competing Interest

The authors declare that they have no known competing financial interests or personal relationships that could have appeared to influence the work reported in this paper.

Acknowledgement

Authors would like to thank Berko İlaç for providing fusidic acid. Also, authors are grateful to Assoc. Prof. Dilek Telci for providing RAW 264.7 macrophage cells.

References

- Altöparlak, U., Erol, S., Akçay, M.N., Celebi, F., Kadanali, A., 2004. The time-related changes of antimicrobial resistance patterns and predominant bacterial profiles of burn wounds and body flora of burned patients. *Burns* 30, 660–664. <https://doi.org/10.1016/j.burns.2004.03.005>.
- Ayla, Ş., Günel, M.Y., Sayın Şakul, A.A., Biçeroğlu, Ö., Özdemir, E.M., Okur, M.E., Polat, D.Ç., Üstündağ Okur, N., Bilgiç, B.E., 2017. Effects of *Prunus spinosa* L. fruits on experimental wound healing. *Medeni. Med. J.* 32, 152–158. <https://doi.org/10.5222/mmj.2017.152>.
- Banerjee, S., Argaez, C., 2017. Topical Antibiotics for Infection Prevention: A Review of the Clinical Effectiveness and Guidelines 1–28.
- Bonamonte, D., Belloni Fortina, A., Neri, L., Patrizi, A., 2014. Fusidic acid in skin infections and infected atopic eczema. *G. Ital. di Dermatologia e Venereol.* 149, 453–459. <https://doi.org/10.1055/s-2004-815600>.
- D'Avignon, L.C., Hogan, B.K., Murray, C.K., Loo, F.L., Hospenthal, D.R., Cancio, L.C., Kim, S.H., Renz, E.M., Barillo, D., Holcomb, J.B., Wade, C.E., Wolf, S.E., 2010. Contribution of bacterial and viral infections to attributable mortality in patients with severe burns: An autopsy series. *Burns* 36, 773–779. <https://doi.org/10.1016/j.burns.2009.11.007>.
- Dai, T., Huang, Y.Y., Sharma, S.K., Hashmi, J.T., Kurup, D.B., Hamblin, M.R., 2010. Topical antimicrobials for burn wound infections. *Recent Pat. Antiinfect. Drug Discov.* 5, 124–151.
- Davaa, E., Park, J.-S., 2012. Formulation parameters influencing the physicochemical characteristics of rosiglitazone-loaded cationic lipid emulsion. *Arch. Pharm. Res.* 35, 1205–1213. <https://doi.org/10.1007/s12272-012-0711-1>.
- Dua, K., Chakravarthi, S., Kumar, D., Sheshala, R., Gupta, G., 2013. Formulation, characterization, *in vitro*, *in vivo*, and histopathological evaluation of transdermal drug delivery containing norfloxacin and *Curcuma longa*. *Int. J. Pharm. Investig.* 3, 183–187. <https://doi.org/10.4103/2230-973X.121287>.
- Froelich, A., Osmalek, T., Kunstman, P., Jadach, B., Brzostowska, M., Białas, W., 2019. Design and study of poloxamer-based microemulsion gels with naproxen. *Colloids Surfaces A Physicochem. Eng. Asp.* 562, 101–112. <https://doi.org/10.1016/j.colsurfa.2018.11.006>.
- Froelich, A., Osmalek, T., Snela, A., Kunstman, P., Jadach, B., Olejniczak, M., Roszak, G., Białas, W., 2017. Novel microemulsion-based gels for topical delivery of indomethacin: Formulation, physicochemical properties and *in vitro* drug release studies. *J. Colloid Interface Sci.* 507, 323–336. <https://doi.org/10.1016/j.jcis.2017.08.011>.
- Galeano, M., Altavilla, D., Bitto, A., Minutoli, L., Calò, M., Cascio, P., Polito, F., Giugliano, G., Squadrito, G., Mioni, C., Giuliani, D., Venuti, F.S., Squadrito, F., 2006. Recombinant human erythropoietin improves angiogenesis and wound healing in experimental burn wounds. *Crit Care Med.* 34, 1139–1146. <https://doi.org/10.1097/01.CCM.0000206468.18653.EC>.
- Ghorbanzadeh, M., Farhadian, N., Golmohammadzadeh, S., Karimi, M., Ebrahimi, M., 2019. Formulation, clinical and histopathological assessment of microemulsion based hydrogel for UV protection of skin. *Colloids Surfaces B Biointerfaces* 179, 393–404. <https://doi.org/10.1016/j.colsurfb.2019.04.015>.
- Gurel, M.S., Nayci, S., Turgut, A.V., Bozkurt, E.R., 2015. Comparison of the effects of topical fusidic acid and rifamycin on wound healing in rats. *Int. Wound J.* 12, 106–110. <https://doi.org/10.1111/iwj.12060>.
- Hajjar, B., Zier, K.-I., Khalid, N., Azarmi, S., Löbenberg, R., 2018. Evaluation of a microemulsion-based gel formulation for topical drug delivery of diclofenac sodium. *J. Pharm. Investig.* 48, 351–362. <https://doi.org/10.1007/s40005-017-0327-7>.
- Hamed, R., Al-Adhami, Y., Abu-Huwajir, R., 2019. Concentration of a microemulsion influences the mechanical properties of ibuprofen in situ microgels. *Int. J. Pharm.* 570. <https://doi.org/10.1016/j.jpharm.2019.118684>.
- Heidari, M., Bahramsoltani, R., Hossein Abdolghaffari, A., Rahimi, R., Esfandiyari, M., Baeeri, M., Hassanzadeh, G., Abdollahi, M., Farzaei, M.H., 2019. Efficacy of topical application of standardized extract of *Tragopogon graminifolius* in the healing process of experimental burn wounds. <https://doi.org/10.1016/j.jtcme.2018.02.002>.
- Kaita, Y., Tarui, T., Yoshino, H., Matsuda, T., Yamaguchi, Y., Nakagawa, T., Asahi, M., Ii, M., 2019. Sufficient therapeutic effect of cryopreserved frozen adipose-derived regenerative cells on burn wounds. <https://doi.org/10.1016/j.reth.2019.01.001>.
- Kaplan, S.L., Hulten, K.G., Gonzalez, B.E., Hammerman, W.A., Lamberth, L., Versalovic, J., Mason, E.O., 2005. Three-year surveillance of community-acquired *Staphylococcus aureus* infections in children. *Clin. Infect. Dis.* 40, 1785–1791. <https://doi.org/10.1086/430312>.
- Kaur, L., Kumar, R., Rahi, D.K., Sinha, V.R., 2018. Formulation and evaluation of microemulsion based gel of voriconazole for topical delivery. *Anti-Infective Agents* 15. <https://doi.org/10.2174/2211352515666170619074437>.
- Kinch, M.S., Patridge, E., Plummer, M., Hoyer, D., 2014. An analysis of FDA-approved drugs for infectious disease: antibacterial agents. *Drug Discov. Today* 19, 1283–1287. <https://doi.org/10.1016/j.drudis.2014.07.005>.
- Lee, D.H., Kim, D.Y., Yoon, S.Y., Park, H.S., Yoon, H.-S., Cho, S., 2015. Retrospective clinical trial of fusidic acid versus petrolatum in the postprocedure care of clean dermatologic procedures. *Ann. Dermatol.* 27, 15–20. <https://doi.org/10.5021/ad.2015.27.1.15>.
- Lipsky, B.A., Hoey, C., 2009. Topical antimicrobial therapy for treating chronic wounds. *Clin. Infect. Dis.* 49, 1541–1549. <https://doi.org/10.1086/644732>.
- Mali, K.K., Dhawale, S.C., Dias, R.J., 2017. Microemulsion based bioadhesive gel of itraconazole using tamarind gum: *in-vitro* and *ex-vivo* evaluation. *Marmara Pharm. J.* 21, 688–700. <https://doi.org/10.12991/marupj.323593>.
- Mehta, D., Rathod, H., Shah, D., Shah, C., 2015. A review on microemulsion based gel: a recent approach for topical drug delivery system. *Res. J. Pharm. Technol.* 8, 118–126. <https://doi.org/10.5958/0974-360X.2015.00021.9>.
- Merchant, N., Smith, K., Jeschke, M.G., 2015. An ounce of prevention saves tons of lives: infection in burns. *Surg. Infect. (Larchmt)* 16, 380–387. <https://doi.org/10.1089/sur.2013.135>.
- Mofazzal Jahromi, M.A., Sahandi Zangabad, P., Moosavi Basri, S.M., Sahandi Zangabad, K., Ghamarypour, A., Aref, A.R., Karimi, M., Hamblin, M.R., 2018. Nanomedicine and advanced technologies for burns: Preventing infection and facilitating wound healing. *Adv. Drug Deliv. Rev.* <https://doi.org/10.1016/j.addr.2017.08.001>.
- Monstrey, S., Hoeksema, H., Verbelen, J., Pirayesh, A., Blondeel, P., 2008. Assessment of burn depth and burn wound healing potential. *Burns* 34, 761–769. <https://doi.org/10.1016/j.burns.2008.01.009>.
- Norbury, W., Herndon, D.N., Tanksley, J., Jeschke, M.G., Finnerty, C.C., 2016. Infection in Burns. *Surg. Infect. (Larchmt)* 17, 250–255. <https://doi.org/10.1089/sur.2013.134>.
- Okur, M.E., Ayla, Ş., Çiçek Polat, D., Günel, M.Y., Yoltaş, A., Biçeroğlu, Ö., 2018. Novel insight into wound healing properties of methanol extract of *Capparis ovata* Desf. var. *palaestina* Zohary fruits. *J. Pharm. Pharmacol.* 70, 1401–1413. <https://doi.org/10.1111/jphp.12977>.
- Olejnik, A., Glowka, A., Nowak, I., 2018. Release studies of undecylenoyl phenylalanine from topical formulations. *Saudi Pharm. J.* 26, 709–718. <https://doi.org/10.1016/j.sjps.2018.02.019>.
- Oryan, A., Jalili, M., Kamali, A., Nikahval, B., 2018. The concurrent use of probiotic microorganism and collagen hydrogel/scaffold enhances burn wound healing: An *in vivo* evaluation. *Burns* 44, 1775–1786. <https://doi.org/10.1016/j.burns.2018.05.016>.
- Reis, R., Sipahi, H., Zeybekoğlu, G., Çelik, N., Kırmızıbekmez, H., Kalkıkaya, N., Aydın, A., 2018. Hydroxytyrosol: the phytochemical responsible for bioactivity of traditionally used olive pits. *Euroasian J. hepato-gastroenterology* 8, 126–132. <https://doi.org/10.5005/jp-journals-10018-1278>.
- Rowan, M.P., Cancio, L.C., Elster, E.A., Burmeister, D.M., Rose, L.F., Natesan, S., Chan, R.K., Christy, R.J., Chung, K.K., 2015. Burn wound healing and treatment: review and advancements. *Crit. Care* 19, 243. <https://doi.org/10.1186/s13054-015-0961-2>.
- Salama, A.A., AbouLaila, M., Moussa, A.A., Nayel, M.A., El-Sify, A., Terkawi, M.A., Hassan, H.Y., Yokoyama, N., Igarashi, I., 2013. Evaluation of *in vitro* and *in vivo* inhibitory effects of fusidic acid on *Babesia* and *Theileria* parasites. *Vet. Parasitol.* 191, 1–10. <https://doi.org/10.1016/j.vetpar.2012.08.022>.
- Schöfer, H., Simonsen, L., 2010. Fusidic acid in dermatology: an updated review. *Eur. J. Dermatol.* 20, 6–15. <https://doi.org/10.1684/EJD.2010.0833>.
- Schulz, G., Stechmiller, J., 2006. Wound healing and nitric oxide production: too little or too much may impair healing and cause chronic wounds. *Int. J. Low. Extrem. Wounds* 5, 6–8. <https://doi.org/10.1177/1534734606286633>.
- Sellimi, S., Maalej, H., Rekiq, M., Benslima, A., Ksouda, G., Hamdi, M., Sahnoun, Z., Li, S., Nasri, M., Hajji, M., 2018. Antioxidant, antibacterial and *in vivo* wound

- healing properties of laminaran purified from *Cystoseira barbata* seaweed. <https://doi.org/10.1016/j.ijbiomac.2018.07.171>.
- Serra, R., Grande, R., Butrico, L., Rossi, A., Settimio, U.F., Caroleo, B., Amato, B., Gallelli, L., de Franciscis, S., 2015. Chronic wound infections: the role of *Pseudomonas aeruginosa* and *Staphylococcus aureus*. *Expert Rev. Anti. Infect. Ther.* 13, 605–613. <https://doi.org/10.1586/14787210.2015.1023291>.
- Sevgi, M., Toklu, A., Vecchio, D., Hamblin, M.R., 2013. Topical antimicrobials for burn infections - an update. *Recent Pat. Antiinfect. Drug Discov.* 8, 161–197.
- Shishoo, C., Chudasama, A., Patel, V., Nivsarkar, M., Vasu, K., 2011. Investigation of microemulsion system for transdermal delivery of itraconazole. *J. Adv. Pharm. Technol. Res.* 2, 30. <https://doi.org/10.4103/2231-4040.79802>.
- Siafaka, P., Okur, M.E., Ayla, Ş., Er, S., Çağlar, E.Ş., Okur, N.Ü., 2019. Design and characterization of nanocarriers loaded with Levofloxacin for enhanced antimicrobial activity; physicochemical properties, in vitro release and oral acute toxicity. *Brazilian J. Pharm. Sci.* 55, 1–13. <https://doi.org/10.1590/s2175-97902019000118295>.
- Siafaka, P.I., Zisi, A.P., Exindari, M.K., Karantas, I.D., Bikiaris, D.N., 2016. Porous dressings of modified chitosan with poly(2-hydroxyethyl acrylate) for topical wound delivery of levofloxacin. *Carbohydr. Polym.* 143, 90–99. <https://doi.org/10.1016/j.carbpol.2016.02.009>.
- Siebenhaar, F., Syska, W., Weller, K., Magerl, M., Zuberbier, T., Metz, M., Maurer, M., 2007. Control of *Pseudomonas aeruginosa* skin infections in mice is mast cell-dependent. *Am. J. Pathol.* 170, 1910–1916. <https://doi.org/10.2353/ajpath.2007.060770>.
- Solans, C., García-Celma, M.J., 1997. Surfactants for microemulsions. *Curr. Opin. Colloid Interface Sci.* 2, 464–471. [https://doi.org/10.1016/S1359-0294\(97\)80093-3](https://doi.org/10.1016/S1359-0294(97)80093-3).
- Szumala, P., 2015. Structure of Microemulsion Formulated with Monoacylglycerols in the Presence of Polyols and Ethanol. *J. Surfactants Deterg.* 18, 97–106. <https://doi.org/10.1007/s11743-014-1618-x>.
- Thakur, K., Sharma, G., Singh, B., Chhibber, S., Patil, A.B., Katare, O.P., 2018. Chitosan-tailored lipidic nanoconstructs of Fusidic acid as promising vehicle for wound infections: An explorative study. *Int. J. Biol. Macromol.* 115, 1012–1025. <https://doi.org/10.1016/j.ijbiomac.2018.04.092>.
- Trabelsi, I., Ktari, N., Ben Slima, S., Triki, M., Bardaa, S., Mnif, H., Ben Salah, R., 2017. Evaluation of dermal wound healing activity and in vitro antibacterial and antioxidant activities of a new exopolysaccharide produced by *Lactobacillus* sp. *Ca 6. Int. J. Biol. Macromol.* 103, 194–201. <https://doi.org/10.1016/j.ijbiomac.2017.05.017>.
- Üstündağ-Okur, N., Ege, M.A., Karasulu, H.Y., 2014a. Preparation and Characterization of Naproxen Loaded Microemulsion Formulations for Dermal Application. *Int. J. Pharm.*
- Üstündağ-Okur, N., Gökçe, E.H., Bozbiyik, D.I., Eğrilmez, S., Özer, Ö., Ertan, G., 2014b. Preparation and in vitro-in vivo evaluation of ofloxacin loaded ophthalmic nano structured lipid carriers modified with chitosan oligosaccharide lactate for the treatment of bacterial keratitis. *Eur. J. Pharm. Sci.* 63, 204–215. <https://doi.org/10.1016/j.ejps.2014.07.013>.
- Üstündağ-Okur, N., Gökçe, E.H., Eğrilmez, S., Özer, Ö., Ertan, G., 2014. Novel ofloxacin-loaded microemulsion formulations for ocular delivery. *J. Ocul. Pharmacol. Ther.* 30, 319–332. <https://doi.org/10.1089/jop.2013.0114>.
- Üstündağ Okur, N., Apaydin, Ş., Karabay Yavaşoğlu, N.Ü., Yavaşoğlu, A., Karasulu, H. Y., 2011. Evaluation of skin permeation and anti-inflammatory and analgesic effects of new naproxen microemulsion formulations. *Int. J. Pharm.* 416, 136–144. <https://doi.org/10.1016/j.ijpharm.2011.06.026>.
- Üstündağ Okur, N., Çağlar, E.Ş., Arpa, M.D., Karasulu, H.Y., 2016a. Preparation and evaluation of novel microemulsion-based hydrogels for dermal delivery of benzocaine. *Pharm. Dev. Technol.* 1–11. <https://doi.org/10.3109/10837450.2015.1131716>.
- Üstündağ Okur, N., Çağlar, E.Ş., Yozgatlı, V., 2016. Development and validation of an HPLC method for voriconazole active substance in bulk and its pharmaceutical formulation. *Marmara Pharm. J.* 20. <https://doi.org/10.12991/mpj.20162076793>.
- Üstündağ Okur, N., Hökenek, N., Okur, M.E., Ayla, Ş., Yoltaş, A., Siafaka, P.I., Cevher, E., 2019a. An alternative approach to wound healing field; new composite films from natural polymers for mupirocin dermal delivery. *Saudi Pharm. J.* 27, 738–752. <https://doi.org/10.1016/j.jsps.2019.04.010>.
- Üstündağ Okur, N., Yavaşoğlu, A., Karasulu, H.Y., 2014. Preparation and evaluation of microemulsion formulations of naproxen for dermal delivery. *Chem. Pharm. Bull. (Tokyo)* 62, 135–143.
- Üstündağ Okur, N., Yozgatlı, V., Okur, M.E., Yoltaş, A., Siafaka, P.I., 2019b. Improving therapeutic efficacy of voriconazole against fungal keratitis: Thermo-sensitive in situ gels as ophthalmic drug carriers. *J. Drug Deliv. Sci. Technol.* 49, 323–333. <https://doi.org/10.1016/j.jddst.2018.12.005>.
- Wang, Y., Beekman, J., Hew, J., Jackson, S., Issler-Fisher, A.C., Parungao, R., Lajevardi, S.S., Li, Z., Maitz, P.K.M., 2018. Burn injury: Challenges and advances in burn wound healing, infection, pain and scarring. *Adv. Drug Deliv. Rev.* 123, 3–17. <https://doi.org/10.1016/j.addr.2017.09.018>.